applied sciences

MDPI

Article

Research of Peak Searching Technology for Separating Lithium from Coal Based on XRD Pattern

Xiaoping Jiang, Yurong Liu * and Tianning Xiu

School of Mechanical Electronic & Information Engineering, China University of Mining and Technology-Beijing, Beijing 100083, China
* Correspondence: liuyr_1024@163.com; Tel.: +86-182-16712956

Abstract: X-ray diffraction technology (XRD) is one of the common means of mineral separation, and peak identification and comparison is a key step. The symmetric zero-area conversion method (SZAC) performs well in peak searching of spectral lines, but its wide application is limited by problems such as inaccurate identification results in specific scenes and dependence of parameter selection on spectral data. In this article, an improved symmetric zero-area conversion method (ISZAC) is proposed by combining the ideas of data fusion and passive anti-counterfeiting. The comparison method and flat peak screening were introduced, and the function group was designed to convert the spectral data after background deduction and intensity screening. The results were fused to obtain the peak address determination. Simulation and experimental results show that the improved method has higher accuracy and applicability. In addition, the method is easy to expand, and the conversion function group can be adjusted according to the spectral data characteristics to improve the recognition efficiency.

Keywords: mineral separation; peak searching; symmetric zero-area conversion method; data fusion; passive anti-counterfeiting

Citation: Jiang, X.; Liu, Y.; Xiu, T. Research of Peak Searching Technology for Separating Lithium from Coal Based on XRD Pattern. *Appl. Sci.* **2023**, *13*, 4016. https://doi.org/10.3390/app13064016

Academic Editor: Arcady Dyskin

Received: 25 February 2023
Revised: 16 March 2023
Accepted: 17 March 2023
Published: 22 March 2023

1. Introduction

Lithium (Li) is one of the rare metals associated with coal, which has extremely high strategic value. Li mining in coal is expected to become an important way to supplement Li [1–5]. XRD is a common phase analysis method, which can be used to identify Li in coal. The diffraction pattern is related to the phase, and different patterns are due to different phases. The phase composition of the sample can be determined by comparing the diffraction pattern with the standard powder diffraction file (PDF), and the location of the diffraction peak is one of the main indicators for comparison [6,7].

Spectral line peak search is the prerequisite of qualitative and quantitative analysis in nuclear, spectral, and chromatographic analysis, and the optimization of peak search algorithms is an inevitable requirement for the development of the spectral analysis field. Common algorithms include the comparison method, derivative method (first order, second order, third order), covariance method, etc. [8–11]. The evaluation of peak searching algorithms mainly focuses on their ability to identify overlapping peaks and weak peaks. By constructing a symmetric "window" function with zero area, used for convolution transformation of the spectral data, and then using threshold screening to determine peak position, SZAC performs well in the above two aspects [12,13].

SZAC was derived from the second derivative method. Pang et al. [14] gave a method to determine the conversion function and compared the peak search effect under different functions. The results show that a "wide" window conversion function can suppress high base and statistical false peaks, and a "narrow" window conversion function can improve the ability to distinguish overlapping peaks. Shang et al. [15] discussed and compared the principles of various peak searching algorithms for X-ray fluorescence spectra, and

confirmed that the Gaussian fitting method and SZAC were ideal algorithms, and SZAC was especially effective in identifying weak peaks superimposed on high substrates. Bi et al. [16] took LIBS/Raman spectra as the research object to explore the recognition effect of peak-like conversion functions constructed by three different linear functions they pointed out that SZAC has strong adaptability to large-scale dynamic changes of signals, and its recognition ability of weak peaks reaches or is better than that of manual recognition. In general, research of SZAC has a certain basis. However, the above studies all analyzed a single determined spectrum and set parameters according to the research object. If the spectral data is changed, the parameters need to be greatly adjusted to achieve a better peak search effect. The strong dependence on the source spectrum and experience results in the limited use and reduced applicability of SZAC. This article aims to obtain an improvement method, ISZAC, by combining multi-source data fusion, which is effective for most of the sample without changing parameters.

This article elaborates the principle of SZAC and analyzes its limitations in two aspects. On the basis of explaining the idea of passive anti-counterfeiting and data fusion, ISZAC is proposed and its implementation steps are analyzed. Finally, the accuracy and applicability of ISZAC are verified by a peak searching experiment, and the actual peak searching effect of ISZAC on lithium in coal XRD patterns is tested.

2. The Symmetric Zero-Area Conversion Method

2.1. The Introduction of SZAC

Window function C needs to satisfy symmetry, and its total area is 0, as shown in Expression (1).

$$\sum_{j=-m}^{m} C_j = 0, C_j = C_{-j} \tag{1}$$

where m is half the window width. In this paper, the peak-like function constructed by the Gaussian function is selected as the window function, and its basic form is shown in Expression (2). H_G is the full width at half maximum (FWHM).

$$C_j = G_j - \frac{\sum_{j=-m}^{m} G_j}{2m+1} \tag{2}$$

$$G_j = e^{-4\ln 2(j/H_G)^2} \tag{3}$$

$$y_i^* = \sum_{j=-m}^{m} C_i y_{i+j} \tag{4}$$

Expression (4) describes the conversion process, y_i is the original spectral data, and y_i^* is the conversion result. Threshold processing is required before peak identification. According to the "3δ" rule, define threshold function as Expression (5).

$$T(i) = \frac{y_i^*}{\delta y^*} \tag{5}$$

$$\delta y^* = \sqrt{\frac{\sum_{i=1}^{n} \left(y_i^* - \bar{y^*}\right)^2}{n}} \tag{6}$$

$$\bar{y^*} = \frac{\sum_{i=1}^{n} y_i^*}{n} \tag{7}$$

where n is the total address number, and δy^* is the standard deviation of y^*. If the address i meets $T(i) > T_0$, it is determined to be the peak, and T_0 is generally set as 1~2.5.

The core idea of SZAC is to process spectral data with sliding window function conversion. According to the characteristics of the window function, the conversion result at the peak value is a large positive number, while the non-peak one is small or even negative. On this basis, the peak position can be identified by filtering the threshold value. The threshold function is linear. Its purpose is to reduce the influence of spectral intensity on the conversion results, and unify the threshold-processing results of different orders of magnitude to the order of T_0.

2.2. The Limitation of SZAC

Analyzing the implementation process of SZAC can find that the conversion results in specific scenes cannot accurately distinguish peak positions. For example, when $m = 1$, the conversion function is denoted as $C = [-c, 2c, -c]$, the original spectral data is $y = [y_1, y_2, y_3]$, and the conversion result while $i = 2$ is shown as Expression (8).

$$y_2^* = (-c) \cdot y_1 + 2c \cdot y_2 + (-c) \cdot y_3 = c(2y_2 - y_1 - y_3) \quad (8)$$

If y_2 is the peak, $y_2 > y_1$, $y_2 > y_3$, then $y_2^* > 0$. If y_2 is not the peak but has the characteristics of $2y_2 - y_1 - y_3 > 0$, the calculation result is still greater than 0. If the result of $2y_2 - y_1 - y_3$ is large enough, the threshold processing result here will be greater than the given threshold, resulting in an error in the judgment result, which is one of the limitations of SZAC.

On the other hand, three parameters, m, H_G, and T_0, need to be set during peak searching with SZAC. One study found that when the peak-like function is similar to the original spectral data, the variation results are optimal. Therefore, the peak type of the original spectral data can be obtained in advance, and H_G can be determined according to its FWHM. The selection of T_0 is appropriate to distinguish the peak position effectively, which has strong dependence on the data. m directly affects the change results. Wide windows can suppress noise, while narrow windows can improve the recognition ability of overlapping peaks. The setting of this parameter depends on the performance requirements of the algorithm. The dependence of parameter selection on spectral data characteristics and experience is another limitation of SZAC.

The above two aspects limit the application scope of SZAC. To reduce or eliminate the influence of limitations and improve the applicability of SZAC is the focus of this paper.

3. The Improved Symmetric Zero-Area Conversion Method

In order to solve the above problems, combined with the passive anti-counterfeiting idea, an improved symmetric zero-area conversion method based on data fusion is proposed. Multiple conversion functions are selected to reduce the influence of the randomness of spectral data and ensure that each conversion result at the peak position is positive. Therefore, when a negative number exists in the result group of an address, the address can be determined as non-peak. The selection of the conversion function group is mainly based on the symmetric zero-area conversion function with different m values. At the same time, it is necessary to introduce a new method to make up for the failure of SZAC in specific scenarios.

3.1. Passive Anti-Counterfeiting and Information Fusion

In recognition of the authenticity of banknotes, a passive anti-counterfeiting method that counts and narrates the feature range of genuine banknotes and determines the banknotes that are not within the range as counterfeit banknotes is widely used [17]. Since both studies are binary problems, this idea is adopted to identify the peak position. The characteristics of spectral data are diverse and their randomness is large, so it is difficult to screen out all types of non-peaks exhaustively. Based on the passive anti-counterfeiting idea, this article uses the feature that the conversion results of peak position are all positive, searches the negative values in the result group of each address to exclude non-peak positions, and effectively improves the identification efficiency of peak positions.

Information fusion refers to synthesizing data from different sources to comprehensively perceive objects and provide support for the final decision [18,19]. In this article, the conversion function group covering the narrow window to the wide window is selected, and the result group is used as the data source for fusion processing. Parameter m does not need to be adjusted according to the spectral data. Using the "and" fusion criterion, the fusion decision is positive when all data sources are true, and zero in other cases. The regionalized fusion result is used to replace the continuous threshold processing result in SZAC, and the identification can be completed by setting the parameter $T_0 = 0$.

3.2. Background Deduction and Intensity Screening

Background refers to other interference factors that cause count in the spectral data except the measured radioactive sources, and it is necessary to conduct deduction processing before peak search [20]. Background deduction methods mainly include Fourier conversion technology, digital filtering technology, statistically sensitive nonlinear iterative peaking algorithm (SNIP), etc. [21,22]. SNIP is simple in principle and fast in calculation. In this article, an improved Simpson–SNIP algorithm is used for background deduction.

(I) In order to reduce the wide variation of each address count [23], the original spectral data is processed according to Expression (9).

$$V(i) = \ln[\ln(\sqrt{y(i)+1}+1)+1] \tag{9}$$

where $y(i)$ represents the count of i address, and $V(i)$ represents the conversion result.

(II) Obtain the full spectrum background iteratively. One study found that if the Simpson formula is used to replace the rectangular formula in the original SNIP algorithm, the calculation results will have higher accuracy [24].

$$V_p(i) = \min\left\{V_{p-1}(i), \frac{1}{6}[V_{p-1}(i-p) + 4V_{p-1}(i) + V_{p-1}(i+p)]\right\} \tag{10}$$

where p represents the number of iterations, $V_p(i)$ represents the iteration result of the p th time, and $V_0(i) = V(i)$.

(III) Using the inverse conversion of Expression (9), the processed data is converted into the original form.

$$y_{SNIP} = \left[e^{e^{V_p(i)}-1} - 1\right]^2 - 1 \tag{11}$$

where y_{SNIP} is the final result of background deduction using the improved Simpson–SNIP algorithm.

Intensity screening of spectral data after background deduction can reduce the calculation amount and improve the precision of peak searching [25,26]. Intensity values based on statistical indicators of spectral data are set, and only data larger than this value are selected for conversion and peak searching [27].

3.3. Comparison Method and Flat Peak Screening

In order to solve the problem of SZAC failure in specific scenes, the comparison method is introduced to ensure that the peak address satisfies the peak characteristics within the left and right *cmpN* access. If the address i is the peak position, Expression (12) must be satisfied.

$$\begin{cases} y_i \geq y_{i+1} \geq y_{i+2} \geq \cdots \geq y_{i+cmpN} \\ y_i \geq y_{i-1} \geq y_{i-2} \geq \cdots \geq y_{i-cmpN} \end{cases} \tag{12}$$

$cmpN$ = 2 is selected to compare the intensity of the two address on both sides of address i, and the relational array $cmpA(i)$ is established.

$$cmpA(i) = [a_{i1}, a_{i2}, a_{i3}, a_{i4}]$$
$$\begin{cases} a_{i1} = \mathrm{sgn}(y_i - y_{i-1}) \\ a_{i2} = \mathrm{sgn}(y_i - y_{i+1}) \\ a_{i3} = \mathrm{sgn}(y_{i-1} - y_{i-2}) \\ a_{i4} = \mathrm{sgn}(y_{i+1} - y_{i+2}) \end{cases} \tag{13}$$

where sgn() is a sign function. If element -1 exists in $cmpA(i)$, then the address i does not meet the peak requirement. For flat peaks with more than one peak width, the search matrix srchM is established, as shown in expression (14).

$$\mathrm{srchM} = \begin{bmatrix} 1,0,1,0 \\ 0,1,0,1 \\ 0,0,1,1 \\ 1,0,1,1 \\ 0,1,1,1 \end{bmatrix} \tag{14}$$

If $cmpA(i)$ is the row element in srchM, then the path address i is the flat peak.

3.4. ISZAC Algorithm

The algorithm flow of ISZAC is shown in Figure 1.

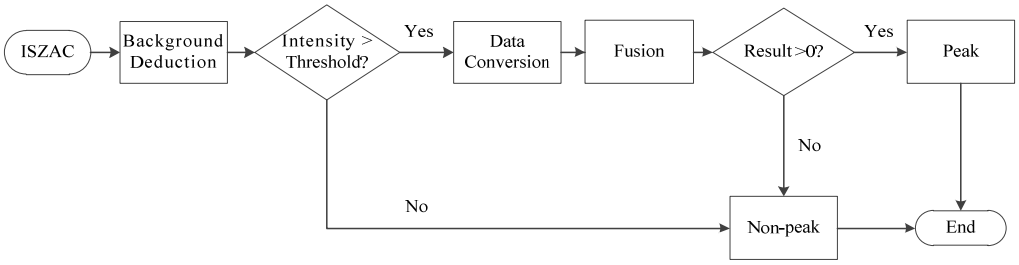

Figure 1. Flow chart of ISZAC algorithm.

(I) Load spectral data and initialize parameters;
(II) Background deduction;
(III) Intensity screening;
(IV) According to the window width range, the symmetric zero-area conversion function is constructed to generate the conversion result group;
(V) According to the comparison width, construct the conversion function of the comparison method, and transmit the conversion results to the next step;
(VI) Flat peak screening, and add results into the result group;
(VII) Fusion processing to generate the final decision result; and
(VIII) Determination of peak position and display of results.

The diagram of data conversion and fusion processing is shown in Figure 2.

The N conversion functions selected are C_1, C_2, ..., C_N, and the corresponding conversion results are y_1^*, y_2^*, ..., y_N^*, the fusion result is y^*, then

$$y^* = \frac{\prod_{i=1}^{N} \mathrm{sgn}(y_i^*) \cdot \prod_{i=1}^{N} \{\mathrm{sgn}(y_i^*) + 1\} \cdot \sum_{i=1}^{N} y_i^*}{N} \tag{15}$$

When there are non-positive numbers in the result group, y^* is 0. When they are all positive, y^* is the average of the sum of conversion results.

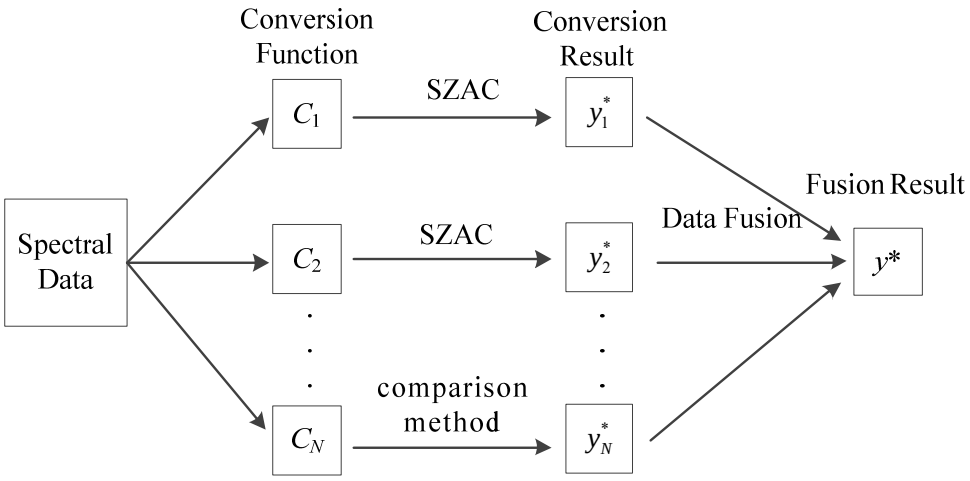

Figure 2. Schematic diagram of data conversion and fusion processing.

The failure of SZAC in a specific scenario is the defect of the method itself. The introduction of a comparison method to correct the judgment results improves one of the limitations of the method. Take m = 2,3,4,5,6, construct a conversion function including narrow window to wide window, and give full play to the ability of overlapping peak recognition and noise suppression. The result of fusion is only 0 and positive, and $T_0 = 0$ can be effectively separated. H_G can be set according to the peak type of input spectral data. Therefore, all three parameters can be determined, which improves SZAC's limitation of relying on data and experience.

In addition, the conversion function group can be adjusted to obtain higher recognition efficiency when searching for peaks of bulk homologous samples with strong similarity. If the FWHM of the target phase peak is small, the comparison function with smaller *cmpN* can be selected to reduce the calculation amount. If there are important peaks with poor recognition effect, a new conversion function can be designed according to the data characteristics of the address to achieve targeted recognition. If the intensity of peak I and its surrounding five address is $y_{[i-2,\, i+2]}$ = [9.8, 10.1, 10.5, 10.2, 10.1], generate the standard Gaussian linear symmetric zero-area conversion function with m = 2, H_G = 4, then C = [−0.24, 0.11, 0.26, 0.11, −0.24], and the result is a small positive value of 0.187. Affected by noise interference or other processing links, the result may be negative, resulting in wrong judgment. Replace C with C^* = [−0.34, 0.11, 0.46, 0.11, −0.34], and the conversion result is 0.297, which has a large margin compared with the original one. ISZAC based on passive anti-counterfeiting only needs the conversion function to meet the characteristics that the conversion result at the peak is greater than 0, there are no strict requirements for symmetry or the sum of conversion function elements is 0. The conversion function group has more possible combinations, which makes ISZAC have good expansibility in engineering practice.

4. Simulation and Experiment

4.1. The Simulation to Verify Accuracy

The simulation waveform is shown in Figure 3, which consists of a strong peak and a weak peak far away from it. The total address number is 90. The peak data were generated by Gaussian linear function, the peak addresses were 51 and 71, and the FWHM were 6 and 4, respectively. The two methods were used to search peaks successively, which verified that ISZAC was superior to SZAC in accuracy. The introduction of the comparison method was able to correct the detection errors of SZAC in specific scenarios.

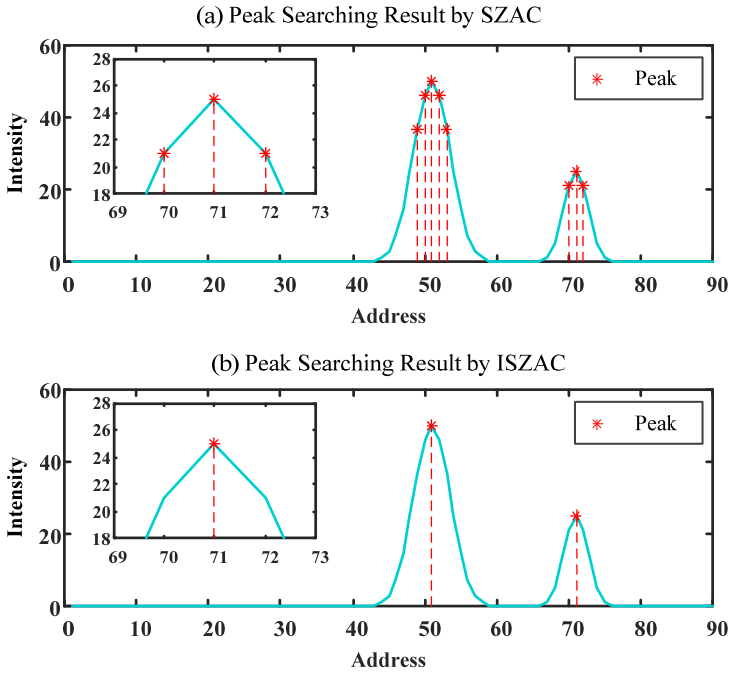

Figure 3. Accuracy verification diagram.

Figure 3a shows the results of SZAC with $m = 2$, $H_G = 4$, and $T_0 = 1.5$. SZAC correctly identified peak addresses 51 and 71, but also misidentified some non-peak addresses as peak. Observe the local magnification map of address 71, note that addresses 70 and 72 do not meet the characteristics of peak and belong to misjudgment results, and analyze the process in detail.

Conversion function $C = [-0.24, 0.11, 0.26, 0.11, -0.24]$. The spectral intensity at address 70 is 21.02, the intensity of the five address around it is $y_{68\text{-}72} = [5.26, 12.50, 21.02, 25.00, 21.02]$, and the conversion result at address 70 is 3.28.

After threshold processing, $T(70) = 2.7 > T_0$, so address 70 is misjudged as the peak, and other misjudged situations are similar.

Figure 3b shows the results of ISZAC, where the conversion function set consists of five Gaussian linear functions with $m = 2, 3, 4, 5, 6$, respectively, and a comparison function with $cmpN = 2$. The H_G of all Gaussian linear function is equal to 6. The number of iterations of background deduction SNIP method is 15. By using ISZAC, misidentified addresses are effectively eliminated.

Derive the result group $rSet(70) = [0.59, 0.55, 0.52, 0.48, 0.46, 1, -1]$ of address 70. The first five values are the results of symmetric zero-area conversion, the sixth value is the result of intensity screening, and the seventh value is the result of the comparison method. By comparing SZAC results, it can be seen that after adjusting parameters m and H_G, the symmetric zero-area conversion result of address 70 is still positive. The key to eliminating address 70 in the subsequent fusion process is that the result of the comparison method is negative. By introducing the comparison method, ISZAC ensures the accuracy of peak identification and improves the limitation of failure of the original SZAC in specific scenarios.

4.2. The Simulation to Verify Applicability and Experimental Test

The simulation waveform is shown in Figure 4, which consists of a strong peak, a sub-strong peak adjacent to the strong peak, and a weak peak far away from them. The total number of addresses is 120. The peak data were generated by Gaussian linear function; the peak addresses were 51, 57, 87; and the FWHM were 6, 4, 6, respectively. Gaussian white noise with SNR = 10dB is added to the data through "awgn" function in MATLAB. Three methods were used to search peaks, respectively, which verified that ISZAC was

superior to SZAC in applicability, and different types of peaks could be identified without modifying parameters.

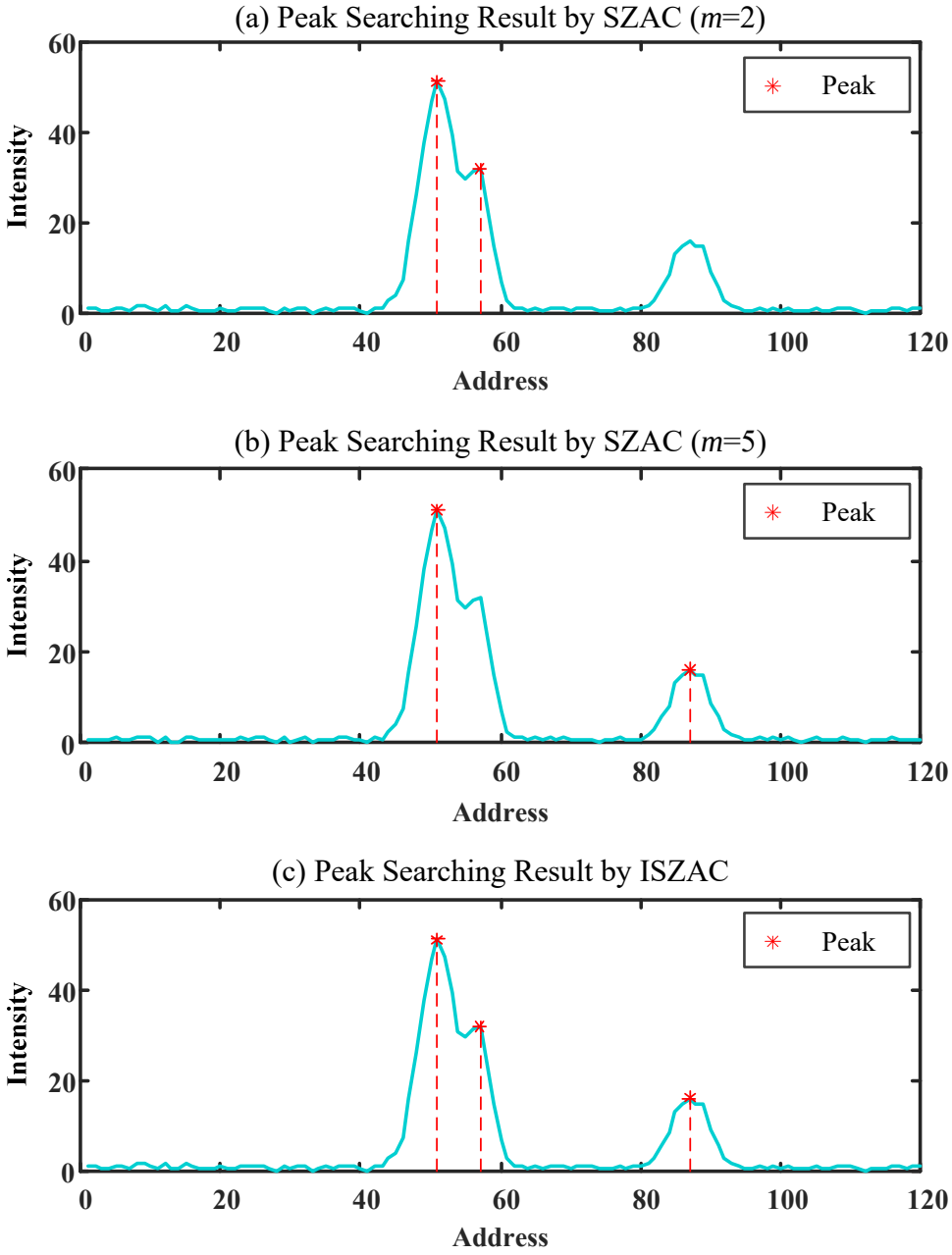

Figure 4. Applicability verification diagram.

Figure 4a shows the results of SZAC with $m = 2$, $H_G = 6$, and $T_0 = 1.5$. The overlapping peak was identified by the narrow window function, but the third peak could not be identified effectively due to the influence of noise. The threshold processing result of the address was $T(87) = 0.75$.

Figure 4b shows the results of SZAC with $m = 5$, $H_G = 6$, and $T_0 = 1.5$. The wide window function is used to identify the third peak affected by noise, but the overlapping peak near the strong peak cannot be effectively identified, and the threshold processing result of this address is $T(57) = 0.99$. In Figure 4a,b, the comparison function with $cmpN = 1$ is introduced to eliminate the misidentification results.

Figure 4c shows the results of ISZAC, and parameter settings are consistent with the aforementioned experiments. The ISZAC method was used to identify the three peaks effectively.

The Narrow window zero-area conversion function has a strong ability to identify overlapping peaks, while the wide window function is beneficial in suppressing noise interference. ISZAC selects multiple conversion functions to give full play to the advantages of each type of conversion function. There is no need to set different parameters according to the input spectrum, which improves the limitation of SZAC parameter setting depending on the spectral data characteristics and experience.

The measured effect of the XRD pattern is shown in Figure 5. The crystal composition of the coal sample includes kaolinite and lithium, with Li accounting for 68.9%. The X-ray diffractometer model is D8, copper target material, voltage 35 KV, current 30 mA, and step size 0.02. Figure 5a shows the results of ISZAC, and the parameter settings are consistent with the above experiments. The peak searching results are basically consistent with the PDF of the two crystal components, and the ISZAC measurement effect is efficient.

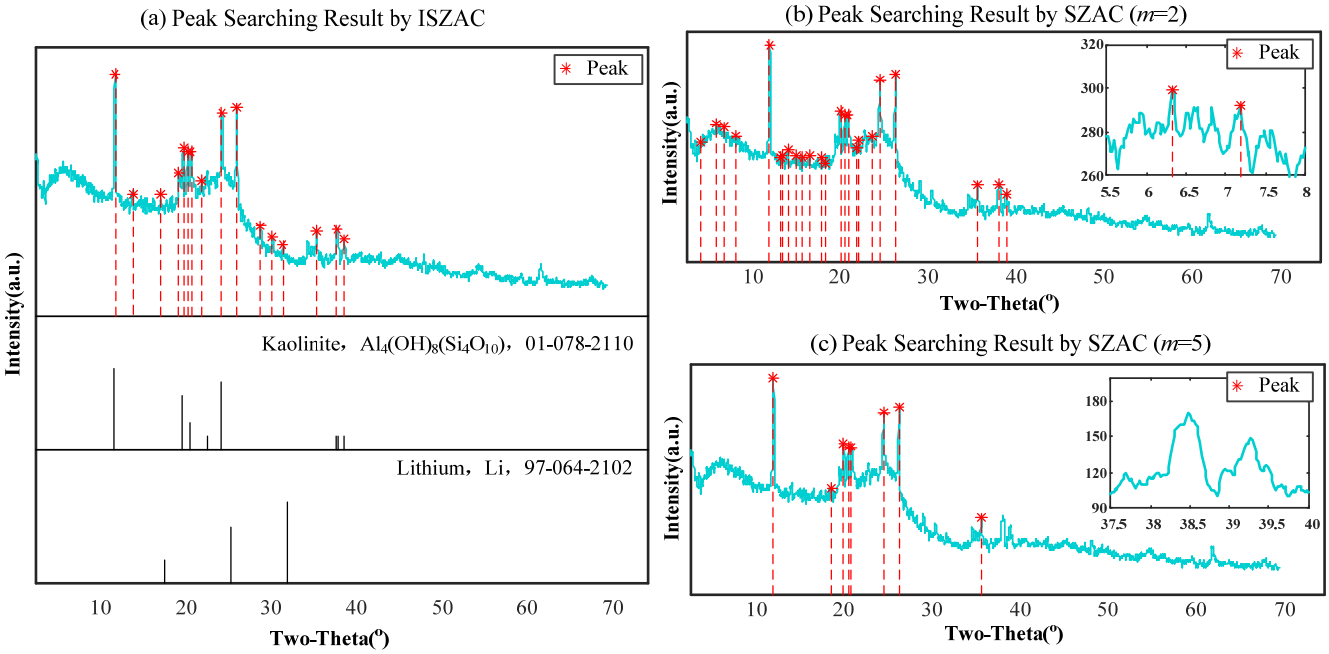

Figure 5. Peak search results of XRD pattern of lithium in coal.

Figure 5b shows the results of SZAC with m = 2, H_G = 6, and T_0 = 2. The number of peaks determined in the recognition result is more than that in the ISZAC, because it misjudges some addresses caused by noise as a peak. Observe the local magnification map of 2θ = [5.5, 8]. The spectral waveform in this range fluctuates greatly, and the peak width at the misidentified address is insufficient. Compared with PDF, it can also be found that there is no peak in this range, and the narrow window function is easily affected by noise, resulting in over-recognition.

Figure 5c shows the results of SZAC with m = 5, H_G = 6, and T_0 = 2. The over-recognition situation is significantly reduced under the wide window function. Observe the local magnification map of 2θ = [37.5, 40] and PDF. There are unrecognized Kaolinite diffraction peaks in this range. The wide window function suppresses the noise interference but causes the phenomenon of missing recognition. It must be pointed out that the comparison function with *cmpN* = 1 is introduced in Figure 5b,c to eliminate the misidentification results.

5. Conclusions and Future Work

The following conclusions can be drawn through simulation verification and experimental testing:

(I) Adjusting parameters cannot correct the misjudgment problem generated by SZAC in specific scenarios. By introducing a comparison method, ISZAC has better accuracy of peak identification.
(II) For different types of spectral signals, SZAC needs to adjust the parameters to achieve the optimal recognition effect, otherwise there will be a phenomenon of missing judgment. ISZAC uses a group of conversion functions to give full play to the advantages of wide and narrow window functions to suppress noise and identify overlapping peaks, which enhances the applicability of the method.
(III) The experimental results of ISZAC basically meet the requirements of phase matching, which has a practical application prospect.

The effect of the SZAC peak search is good, but its two limitations lead to the limited use of the method. Based on the symmetric zero-area conversion, ISZAC introduces a comparison method and data fusion, which improves the accuracy and applicability, and realizes the peak searching of different spectral data under the same set of parameters. In addition, the free combination of conversion functions means ISZAC has good expansibility. The form of the conversion function group can be modified to identify specific samples, so as to obtain higher recognition efficiency. It should be pointed out that the identification results of ISZAC may contain false peaks that meet the peak characteristics. How to adjust the fusion strategy or optimize the method combined with the peak area needs to be further explored in this field.

Author Contributions: Conceptualization, X.J. and Y.L.; methodology, X.J., Y.L. and T.X.; software, X.J., Y.L. and T.X.; validation, X.J. and Y.L.; formal analysis, X.J. and T.X.; investigation, X.J., Y.L. and T.X.; resources, T.X.; data curation, T.X.; writing—original draft preparation, X.J.; writing—review and editing, X.J., Y.L. and T.X.; visualization, Y.L. and T.X.; supervision, X.J.; project administration, Y.L. and T.X.; funding acquisition, T.X. All authors have read and agreed to the published version of the manuscript.

Funding: This work was funded by the National Key Research and Development Program of China (No. 2021YFC2902605).

Institutional Review Board Statement: Not applicable.

Informed Consent Statement: Not applicable.

Data Availability Statement: Data sharing is not applicable to this article.

Conflicts of Interest: The authors declare no conflict of interest.

References

1. Seredin, V.V.; Dai, S.; Sun, Y.; Chekryzhov, I.Y. Coal deposits as promising sources of rare metals for alternative power and energy-efficient technologies. *Appl. Geochem.* **2013**, *31*, 1–11. [CrossRef]
2. Dai, S.; Finkelman, R.B. Coal as a promising source of critical elements: Progress and future prospects. *Int. J. Coal Geol.* **2018**, *186*, 155–164. [CrossRef]
3. Dai, S.; Yan, X.; Ward, C.R.; Hower, J.C.; Zhao, L.; Wang, X.; Zhao, L.; Ren, D.; Finkelman, R.B. Valuable elements in Chinese coals: A review. *Int. Geol. Rev.* **2018**, *60*, 590–620. [CrossRef]
4. Dai, S.; Finkelman, R.B.; French, D.; Hower, J.C.; Graham, I.T.; Zhao, F. Modes of occurrence of elements in coal: A critical evaluation. *Earth-Sci. Rev.* **2021**, *222*, 103815. [CrossRef]
5. Benson, T.R.; Coble, M.A.; Rytuba, J.J.; Mahood, G.A. Lithium enrichment in intracontinental rhyolite magmas leads to Li deposits in caldera basins. *Nat. Commun.* **2017**, *8*, 270. [CrossRef]
6. Coelho, A.A. An indexing algorithm independent of peak position extraction for X-ray powder diffraction patterns. *J. Appl. Crystallogr.* **2017**, *50*, 1323–1330. [CrossRef]
7. Ladd, M.; Palmer, R. *Structure Determination by X-ray Crystallography: Analysis by X-rays and Neutrons*; Springer: Berlin, Germany, 2013; ISBN 978-1-4614-3956-1.
8. Huang, Y.; Liu, M.; Liu, X.; Luo, R. Nuclide spectrum peak searching algorithm based on multiple morphological structuring elements. *J. Phys. Conf. Ser.* **2020**, *1634*, 12078. [CrossRef]
9. Chen, Y.; Yang, X.; Liu, H.-L.; Yang, K.; Zhang, Y.-L. Processing FBG Sensing Signals with Exponent Modified Gaussian Curve Fitting Peak Detection Method. *J. Spectrosc. Spectr. Anal.* **2016**, *36*, 1526–1531. [PubMed]

10. Wu, H.X.; Zhang, H.Q.; Liu, Q.C.; Yang, B.; Wei, Q.; Yuan, X. Information retrieval methods for high resolution gamma-ray spectra. *Nucl. Sci. Technol.* **2012**, *23*, 332–336. [CrossRef]
11. Wu, S.; Tang, X.; Gong, P.; Wang, P.; Liang, D.; Li, Y.; Zhou, C.; Zhu, X. Peak-searching method for low count rate γ spectrum under short-time measurement based on a generative adversarial network. *Nucl. Instrum. Methods Phys. Res. Sect. A Accel. Spectrometers Detect. Assoc. Equip.* **2021**, *1002*, 165262. [CrossRef]
12. Bi, Y.F.; Li, Y.; Du, Z.F.; Chen, L.; Zheng, R.E. Automatic recognition of overlapping spectral peaks by symmetric zero-area conversion combined with L-M fitting. *J. Spectrosc. Spectr. Anal.* **2015**, *35*, 2339–2342.
13. Wang, Y.; Wei, Y. Implicit FWHM calibration for gamma-ray spectra. *Nucl. Sci. Technol.* **2013**, *24*, 59–64. [CrossRef]
14. Pang, J.S.; Zheng, G.F.; Hou, X.F. Finding peak by symmetrical zero area conversion method. *J. At. Energy Sci. Technol.* **1987**, *21*, 270–279.
15. Shang, F.J.; Wang, H.X.; Zhou, R.S. Discussion and practice of peak search algorithm in X fluorescence spectrum analysis. *J. Comput. Tech. Geophys. Geochem. Explor.* **2000**, 364–368.
16. Bi, Y.F.; Li, Y.; Zheng, R.E. The Symmetric Zero-Area Conversion Adaptive Peak-Seeking Method Research for LIBS/Raman Spectra. *Spectrosc. Spectr. Anal.* **2013**, *33*, 438–443. [CrossRef]
17. Lee, J.W.; Gil Hong, H.; Kim, K.W.; Park, K.R. A Survey on Banknote Recognition Methods by Various Sensors. *Sensors* **2017**, *17*, 313. [CrossRef] [PubMed]
18. Hang, Z.; Wangliang, L.; Chuang, L.; Linda, S.; Kaiyan, W. Discussion on multi-sensor information fusion in green house detection system. In Proceedings of the 2017 International Conference on Smart Grid and Electrical Automation, Changsha, China, 27–28 May 2017; pp. 64–67.
19. Li, Y.; Zhao, M.; Xu, M.; Liu, Y.; Qian, Y. Analysis and Comparison of Multi-Source Information Fusion Technologies. In *Frontiers in Artificial Intelligence and Applications*; IOS Press: Amsterdam, The Netherlands, 2019; pp. 1057–1063.
20. Zeng, M.X.; Song, Y.G. Study on Factors Influencing quantitative Analysis of X-ray diffraction phase based on McQuart Algo-rithm. *J. Rock Ore Test.* **2012**, *31*, 798–806.
21. Tomoyori, K.; Hirano, Y.; Kurihara, K.; Tamada, T. Background elimination using the SNIP algorithm for Bragg reflections from a protein crystal measured by a TOF single-crystal neutron diffractometer. *J. Phys. Conf. Ser.* **2016**, *664*, 072049. [CrossRef]
22. He, J.; Xiao, H.; Yang, Y.; Qu, J.; Xu, H.; Lin, L. A study of background subtraction method for NaI(TI) instrument spectrum based on adaptive FWHM. In *AER-Advances in Engineering Research*; Cheng, B., Liang, W., Eds.; Atlantis Press: Berlin, Germany, 2015; pp. 462–468.
23. Wu, H.X.; Liu, Q.C.; Yang, B.; Liu, Y.J. Application of SNIP method in natural radionuclide γ spectrum analysis. *J. Nucl. Technol.* **2010**, *33*, 513–516.
24. Jin, Y.; Fei, L.; Liangquan, G.; Qingxian, Z.; Maolin, X.; Kun, S.; Yi, G. Application of Improved Simpson-Snip Algorithm in spectral Background Deduction for airborne γ Instruments. *J. Nucl. Technol.* **2020**, *43*, 77–83.
25. Song, F.; Sun, W.; Wei, J.; Jiang, M.; Zhang, L.; Zhang, F.; Sui, Q.; Tian, Y. The optimization study of FBG Gaussian fitting peak-detection based on Levenberg-Marquardt Algorithm. In Proceedings of the Chinese Automation Congress, Jinan, China, 20–22 October 2017; pp. 3723–3727.
26. Liu, Q.; Cai, L.J.; Li, Z.Y.; Tang, Z.; Du, F.; Zhao, M. Research on peak-detection algorithm for high-speed and high-precision FBG Demodulation. *Op-Toelectronics Laser* **2012**, *23*, 1233–1239. [CrossRef]
27. Chen, Z.J.; Bai, J.; Wu, Z.T.; Zhao, X.; Zhang, J. Optimization and comparison of Optical Fiber Bragg Grating Reflection Spectrum peak Search Algorithm. *J. Acta Photonica Sin.* **2015**, *44*, 83–88.